



Field validation on vibration control of a cable-stayed footbridge with tuned mass dampers

Qing Wen¹, Xu-gang Hua², and Zheng-qing Chen³

- 1 PhD Candidate, Wind Engineering Research Centre, College of Civil Engineering, Hunan University, Changsha, China. E-mail: wenqing_hn@1261.com
- 2 Professor, Wind Engineering Research Centre, College of Civil Engineering, Hunan University, Changsha, China (Corresponding author). E-mail: cexghua@hotmail.com
- 3 Professor, Wind Engineering Research Centre, College of Civil Engineering, Hunan University, Changsha, China. E-mail: zqchen@hnu.edu.cn

ABSTRACT

This paper presents the field validation of vibration control of a long-span cable-stayed bridge with tuned mass dampers (TMDs). The studied bridge is a separated two-level cable-stayed bridge supported by the same pylon. The lower level is a concrete roadway for traffic while the S-shaped upper level is a steel footbridge. The main span of the bridge is 200m with two side span of 100m. Several steel braces linking the roadway and footbridge decks are installed to increase the stiffness and tuned mass dampers are also designed to increase the damping of target modes. The dynamic parameters of the bridge in vertical and lateral directions are obtained by ambient vibration and jump excitation by crowds. A shaker is further used to achieve the steady-state vibration, where the modal frequency, damping ratio and modal mass are identified. The tuned mass dampers are finely tuned to achieve their optimal design parameters based on the measured frequencies and modal masses. Crowds tests conducted after installation of TMD confirm the validity of TMD in reducing the human-induced lateral and vertical vibrations. Lessons learned from the dynamic tests are also highlighted.

KEYWORDS: *Footbridges, human-induced vibration, tuned mass dampers, dynamic tests.*

1. INTRODUCTION

With the great advances in building materials, construction techniques and design methods accompanied by the aesthetic requirements for greater slenderness, the modern footbridges tend to greater span, lighter weight, and smaller damping. As a consequence, they are more susceptible to vibrations under dynamic loads induced by moving pedestrians (Zivanovic et al. 2005; Chen and Hua 2009). If the footbridge has a natural frequency close to the critical frequencies of dynamic foot loads, resonance can potentially be induced by pedestrians. Shifting the natural frequencies far away from the critical frequencies range is a method to avoid large-amplitude human-induced vibration, which is termed as the frequency adjustment method. However, this method is often not economical, and is difficult to implement for long-span footbridges. Supplementary damping by adding passive energy dissipation devices to the footbridges has been a popular approach to suppress undesirable resonant vibrations. Two commonly used energy dissipation devices are fluid-viscous dampers and tuned mass dampers (TMD) (Soong and Dargush 1997). The first type relies on the relative movements of both ends of the dampers, and is therefore connected between two locations of a structure. TMD is inertial device that is attached to a single location of a structure. TMD has been widely for control of human-induced vibration of long-span footbridges (Fijino et al. 1993; Dallard et al. 2001; Caetano et al. 2010a, 2010b; Bruno et al. 2012).

Traditional TMD usually adopts the fluid viscous damper as a damping element. This damping element could improve the TMD activation acceleration, due to the inner friction force of the damping element. On the other hand, the TMD for controlling lateral human-induced vibration is often required to play a role when the displacement of the footbridge is in millimeter level. Eddy current damping is a non-contact, non-additional stiffness and non-mechanical friction damping device. By adopting eddy current damping as the damping element of TMD, the activation acceleration of TMD will be reduce and no additional stiffness will be introduced. The foundation and application of the eddy current TMD were studied by wind engineering research center of Hunan University (Chen et al. 2013; Wang and Chen. 2013), which indicates that the eddy current TMD is suitable to suppress the human-induced lateral vibration (Wang et al. 2014).

The construction of a curved cable-stayed bridge with main span of 200m in Minyang city, China has motivated the dynamic assessment of human-induced vibrations and development of vibration control strategy. The

distinctive feature of the bridge is the twin-deck systems for the vehicles and pedestrians. This special configuration allows the development of a hybrid control system that combines the steel link beams for improving structural stiffness and TMDs for enhancing the damping ratio of critical modes. This paper presents the field validation of human-induced vibration control of this bridge using eddy current TMDs.

2. DESCRIPTION OF THE MINYANG FIRST BRIDGE

The Minyang First Bridge is located across the Fujiang in the Chengnan New District of Minyang, China. It is a cable-stayed bridge with central span of 200m and two side spans of 100m. In order to meet the requirement of high pedestrian densities at this leisure area, two separate girder systems are designed for vehicles and pedestrians. Therefore, the bridge may be regarded as two cable-stayed bridges sharing the joint same inverted-Y pylons. The road bridge for vehicles has a concrete box-girder of 28m width and 3m height, and the footbridge for pedestrians has a steel box-girder of 6m width and 2m height. The footbridge deck is located above the road bridge deck in elevation, and it roughly follows a shallow letter S in plan such that it goes through the road bridge from one side of road deck to the other side at the central span. Each of the bridge girders is supported by its individual cable systems. Figure 1.1 shows the general view of the Minyang First Bridge.



Figure 2.1 General view of the Mianyang First Bridge

3 DESIGN OF VIBRATION CONTROL SYSTEM

Given the special configuration of the bridge, a hybrid control strategy of the stiffness upgrade and damping enhancement is adopted for the present footbridge. First, three pairs of steel link beams are employed to connect the vehicle deck and pedestrian deck, which improves the stiffness of footbridge to reduce the number of lively modes. A pair of vertical link and a pair of inclined link are installed at the main span, and a pair of the horizontal link is installed at both side spans, as shown in Figure 3.1. Each steel link beam consists of a steel pipe with a diameter of 426 mm and a thickness of 8 mm and a high damping rubber pad of 80mm thick at both ends. The rubber pad is designed such that the connections between the link beam and girder have independent rotational DOFs but the same translational DOFs, and it is also helpful to isolate the vibration of vehicle deck induced by traffic. The link beam is prestressed using the high-strength strands inside steel pipe to guarantee it is in compression. The link beam is modeled as a series system of steel pipe and two 80mm-thick rubber pads for accounting for the limited axial stiffness of rubber pads.

The modal properties are predicted by finite element model with steel link beams, as shown in Figure 3.2. Based on those modal parameters, a simplified dynamic simulation by a mode-by-mode approach is performed to evaluate the maximum acceleration in frequency domain. An exceptionally high density of pedestrian on the footbridge of $1.0\text{p}/\text{m}^2$ was considered. With the length and width of footbridge deck being 400m and 6m, the total number of pedestrians at the design density is 2400. Following the design guideline for steel footbridges (EN03 2007), the equivalent number of synchronized pedestrians is obtained as $n^2=91$ ($=1.85 \times n^{1/2}$). A damping ratio of 0.5% is adopted for every mode. By using modal analysis of single degree of freedom (SDOF), the vertical and lateral maximum accelerations for the lively modes are estimated, as listed in Table 3.1. It should be noted that synchronization lateral excitation for the lateral modes, as also known as the lateral lock-in phenomenon, should be avoided. Based on the Dallard Formula, the critical number of pedestrians for triggering the lateral lock-in for the first lateral mode is 142 for the main span, or equivalently 284 for the whole span. That corresponds to a pedestrian density of $0.12\text{p}/\text{m}^2$, which is much smaller than the designed density of $1.0\text{p}/\text{m}^2$.

To enhance the damping of the lively five modes, then, eddy current TMDs are used. As the minimum damping ratios for avoiding the lateral 'lock-in' for the lateral mode is higher than those for vertical modes, a mass ratios of 3% is used for the lateral mode and a mass ratio of 2% for the vertical modes. After determining the mass

ratios, the optimum parameters for each TMD are determined from the classical theory (Soong and Dargush 1997), as listed in Table 3.2. The locations of each TMD are shown in Figure 3.1.

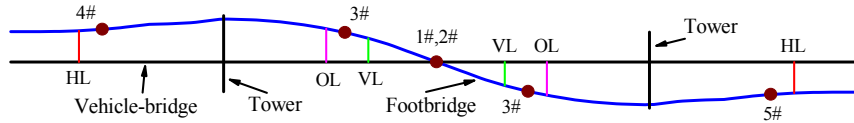


Figure 3.1 Layout of steel link beams and TMDs: HL, OL and VL is horizontal, oblique and vertical link; 1# to 5# are the TMDs for control the 4th, 8th, 14th, 9th and 10th mode respectively.

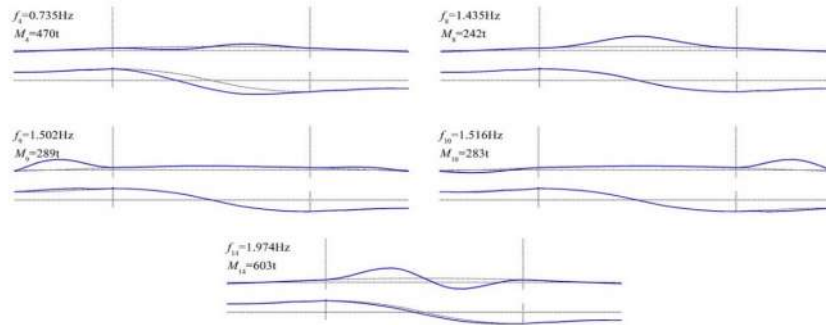


Figure 3.2 Modal properties with steel link beams (the top is elevation view and the bottom is plan view)

Table 3.1 Main modal properties and human-induced vibration of the footbridge with steel link beams

| Mode No. | Natural frequency (Hz) | Modal mass (tons) | Vertical acceleration (m/s ²) | Lateral acceleration (m/s ²) |
|----------|------------------------|-------------------|---|--|
| 4 | 0.735 | 470 | 0.01 | 0.190 |
| 8 | 1.435 | 242 | 1.692 | 0.032 |
| 9 | 1.502 | 289 | 1.741 | 0.271 |
| 10 | 1.516 | 283 | 1.752 | 0.245 |
| 14 | 1.974 | 603 | 1.289 | 0.130 |

Table 3.2 Optimum parameters of TMD for each mode at design stage

| Mode No. | Weight sliding mass (tons) | Frequency (Hz) | Damping ratio (%) | Direction | Locations |
|----------|----------------------------|----------------|-------------------|------------|---------------|
| 4 | 14.0 | 0.714 | 10.5 | Horizontal | 1/2 main span |
| 8 | 5.0 | 1.406 | 8.6 | Vertical | 1/2 main span |
| 9 | 6.0 | 1.472 | 8.6 | Vertical | 1/2 side span |
| 10 | 6.0 | 1.486 | 8.6 | Vertical | 1/2 side span |
| 14 | 12.0 | 1.974 | 8.6 | Vertical | 1/4 main span |

4. EXPERIMENTAL ASSESSMENT OF DYNAMIC BEHAVIORS

A series of dynamic tests are carried out to identify modal parameters of the bridge for fine tuning of tuned mass dampers as well as to evaluate the lateral and vertical vibration response to different pedestrian streams. The first dynamic tests, including ambient vibrations tests and human-induced vibrations tests, are conducted shortly after installation of the three pairs of link beams and before installation of TMDs. The derived results serve for the detailed parameter design of tuned mass dampers as well as for verifying the effectiveness of the link beams. After the final installation of TMDs, the second dynamic tests are carried out. Apart from performing ambient vibration, free vibration tests and human-induced vibration tests, the forced vibration tests by means of a horizontal shaker is also used for the lateral mode.

4.1. Modal Parameters Identification

Many techniques are available to extract modal parameters from ambient vibration responses of a structure in frequency domain or time domain. In this study, the methods used for ambient vibration tests are peak-picking method (PP) (Bendat 1993), enhanced frequency domain decomposition (EFDD) (Brincker and Andersen 2001), stochastic subspace identification method (SSI) (Van and De M 1996). The modal frequencies and damping ratios identified with the above three methods during the first tests are summarized in Table 4.1.

Table 4.1 Summary of identified modal frequencies and damping ratio during the first tests

| Mode No. | FE (with link beams) | | | PP | EFDD | | SSI | |
|----------|----------------------|---------|------------|----------|----------|-------------|----------|-------------|
| | f (Hz) | M (t) | Mode shape | f (Hz) | f (Hz) | ζ (%) | f (Hz) | ζ (%) |
| 4 | 0.734 | 470 | L-S | 0.754 | 0.754 | 0.74 | 0.754 | 0.60 |
| 8 | 1.435 | 242 | V-S | 1.416 | 1.418 | 0.38 | 1.414 | 0.37 |
| 9 | 1.502 | 289 | V-S (side) | 1.669 | 1.669 | \ | 1.664 | 1.10 |
| 10 | 1.516 | 283 | V-S (side) | 1.691 | 1.718 | \ | 1.724 | 2.55 |
| 14 | 1.975 | 603 | V-A | 2.243 | 2.243 | 0.14 | 2.240 | 0.12 |

(Note: V—vertical, L—lateral, S—symmetric, A—Asymmetric)

During the execution of the second dynamics tests, TMDs have been installed inside the box girder of footbridge. In order to obtain the refined estimation of natural frequencies, the motion of mass block is restricted such that the effect of TMD on natural frequencies is merely as the additional weight. The above three techniques are again applied for exacting modal properties of the footbridge from ambient vibration data. In order to estimate the damping ratios more reliably, free decay vibration tests are conducted. Forced vibration test is carried out by means of a horizontal shaker to estimate the modal mass of the first lateral mode. The modal parameters identified by the aforementioned methods are given in Table 4.2.

Table 4.2 Selected experimental modal parameters during the second period tests

| Mode No. | PP | EFDD | SSI | | Free vibration | | Forced vibration | | |
|----------|----------|----------|----------|-------------|----------------|-------------|------------------|-------------|-----------|
| | f (Hz) | f (Hz) | f (Hz) | ζ (%) | f (Hz) | ζ (%) | f (Hz) | ζ (%) | M (ton) |
| 4 | 0.754 | 0.722 | 0.715 | 0.76 | 0.723 | 0.63 | 0.723 | 0.63 | 519 |
| 8 | 1.416 | 1.371 | 1.362 | 1.81 | \ | \ | \ | \ | \ |
| 9 | 1.669 | 1.582 | 1.586 | 1.00 | 1.567 | 1.10 | \ | \ | \ |
| 10 | 1.691 | 1.640 | 1.637 | 0.62 | 1.618 | 0.30 | \ | \ | \ |
| 14 | 2.243 | 2.243 | 2.240 | 0.12 | \ | \ | \ | \ | \ |

The natural frequencies estimated by the second period tests are slightly smaller than the ones by the first period tests, due to the additional mass of the TMDs. The modal mass of the first lateral mode predicted from finite element model of the bridge with additional weight of TMD is 513t. The close agreement between analysis and experiments suggests that the modal mass from finite element analysis is reliable. The modal properties obtained at the second dynamic tests provide the baseline for the design of TMD for the five modes.

4.2. Assessment of Human-Induced Vibrations

During the first dynamic tests, the actual human-induced responses of the footbridge in lateral and vertical directions are assessed by means of pedestrian group tests. Pedestrians circulated anti-clockwise around the main span with an increasing and controlled number up to a maximum of 200 persons. The lateral and vertical acceleration responses at mid-span are recorded, as shown in Figure 4.1. The maximum lateral response is about 0.03m/s^2 for 100 persons walking in main span. The lateral acceleration suddenly increases to 0.2m/s^2 when the number of pedestrian on the main span is 150, suggesting the development of synchronization lateral excitation. The test was forced to stop because the pedestrian paces stopped or were disordered by some pedestrians' panic when the lateral acceleration is up to 0.4m/s^2 for 200 pedestrians. Based on the modal mass (470ton) and damping ratio (0.6%) for the first lateral mode, the theoretical lock-in triggering number of pedestrians in the main span is about 170 person. The triggering number obtained by the tests is generally in good agreement with the theoretical one. The small deviation may be caused the error in damping ratio. The vertical response of the footbridge is considerably less than the predicted one under the same pedestrian number before lateral 'lock-in'.

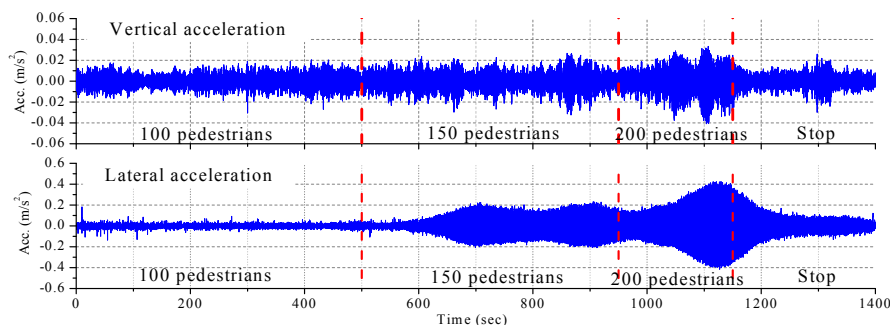


Figure 4.1 Vertical and lateral acceleration response of the mid-span to pedestrian streams

5. FIELD VALIDATION OF TMD PERFORMANCE

5.1. Adjustment of Eddy Current TMD

All TMDs are manufactured based on modal parameters estimated by the first tests, which are slightly different from the ones estimated by the second tests. The modal properties obtained at the second tests provide the baseline for adjustment of TMD for the five modes. However they correspond to the bridge with additional weight caused by the locked TMD. Another important consideration is that the best performance of TMD should be achieved when the footbridge is loaded with a high pedestrian density rather than the empty bridge. After taking into account above effects, the final modal properties of the footbridge used for TMD design are summarized in Table 5.1. The optimal TMD parameters are also listed in Table 5.1. The frequencies of TMDs are tuned by adding or removing the mass as required, and the damping ratios are adjusted by change the gaps between the conductor plates and the magnetic bodies. For practical reasons, each TMD are split into several TMD units which are placed as much as possible close to anti-node for the controlled mode. For example, there are 16 TMD units for lateral TMD and the effective mass for each TMD unit is 875kg, totally amounting up to 14ton as required. Figure 5.1 shows the vertical TMD units and the coupled horizontal and vertical TMD units.

Table 5.1 The modal parameters for the TMD design and basic parameters of TMDs

| Mode No. | Modal parameters of the bridge | | Basic parameters of TMDs | | | |
|----------|--------------------------------|-----------|--------------------------|----------|-----------------|-------------------|
| | f_s (Hz) | M (ton) | μ | f (Hz) | m_{tmd} (ton) | ζ_{tmd} (%) |
| 4 | 0.74 | 470 | 0.03 | 0.718 | 14.0 | 10.6 |
| 8 | 1.41 | 242 | 0.02 | 1.382 | 5.0 | 8.6 |
| 9 | 1.64 | 289 | 0.05 | 1.561 | 13.2 | 13.6 |
| 10 | 1.70 | 283 | 0.05 | 1.619 | 13.2 | 13.6 |
| 14 | 2.05 | 603 | 0.02 | 2.010 | 14.7 | 8.6 |



Figure 5.1 The vertical and the coupled lateral and vertical tuned mass dampers

5.2. Activation of the TMDs

The TMD will be activated when the acceleration of the TMD’s mass exceeds a threshold value to overcome the inevitable friction force between the guide systems. To guarantee the footbridge meet the requirements of comfort, the activation acceleration must be smaller than the comfort limit. For example, tuned mass dampers must take effect when the acceleration is above $0.1m/s^2$ for lateral direction, which is a threshold for triggering synchronization lateral excitation.

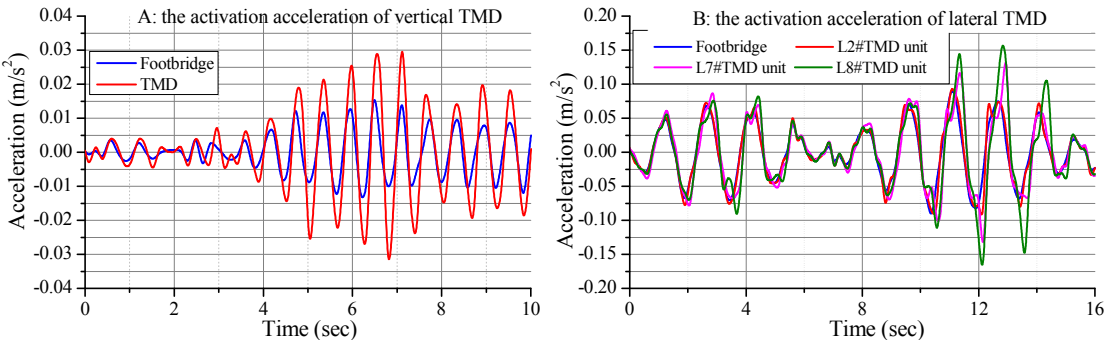


Figure 5.2 Activation acceleration for vertical and lateral TMD units

Figure 5.2 shows the typical acceleration response of the bridge and TMD units. For vertical TMD, as the mass is supported by the springs, the friction force between the guide systems is very small. Therefore, the activation acceleration is very small, as shown in Figure 5.2(A), which is about 0.003m/s^2 . For the lateral TMD, the mass is supported by two rods and it slides along the two rods. To minimize the friction force, the two rods must be installed with accurate leveling and the coefficient of static friction must be as small as possible. If the rods were installed with accurate leveling, the activation acceleration is equivalent to the coefficient of static friction multiplied by gravitational acceleration. The theoretical coefficient of friction for the rods is about $0.002\sim 0.003$. By the dynamic test, the intermittent activation of three lateral TMD units was observed, as shown in Figure 5.2 (B). It can be seen that the two TMD units were activated when the acceleration of footbridge is larger than about 0.06m/s^2 . The activation acceleration for L2#TMD is 0.12m/s^2 .

5.3. Assessment of TMDs Performance

Due to error in manufacture, installation and frequency tuning of TMD, not all TMD units will have the same characteristics, which may attenuate the TMD performance. Figure 5.3 shows the recorded lateral acceleration responses for the selected TMD units and the footbridge induced by the stream of 250 pedestrians after lateral 'lock-in'. It is shown that TMD unit 7 and TMD unit 8 behave almost identically while TMD unit 2 does not operate properly. Under the crowd exciting, the responses of TMD units are not sinusoidal, which indicates the nonlinear properties of the TMD. Due to the differences between units and the nonlinear properties of the TMD, the efficiency of the lateral TMD would be reduced.

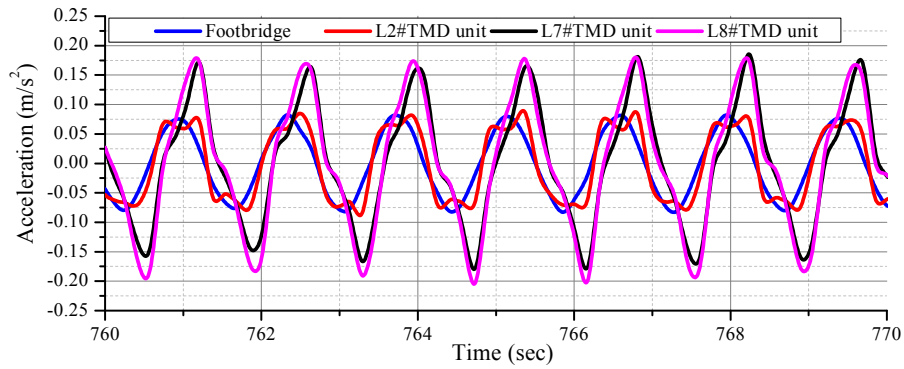


Figure 5.3 The recorded TMD and footbridge accelerations induced by 250 pedestrian

For the vertical TMD, the inherent damping is very low and the required damping are mainly supplied by eddy current damping; for the lateral TMD, the required damping are contributed by both the friction and eddy current damping. It is used to roughly estimate the equivalent damping ratio due to friction, as follows:

$$\zeta_{eq} = \frac{2\kappa g}{\pi\omega^2 u_0} = \frac{2\kappa g}{\pi\dot{u}_0} \quad (5.1)$$

where κ is the measured total kinetic coefficient of friction and $\kappa=0.006$, g is the acceleration of gravity, and u_0 is the displacement amplitude of the TMD. The equivalent damping ratio due to friction is about 19.0% for the acceleration of TMD being 0.2m/s^2 . If the acceleration of footbridge increase to 0.1m/s^2 , the acceleration of TMD would be larger than 0.33m/s^2 , so the equivalent damping ratio due to friction is less than 11.0%. Therefore, before the acceleration of footbridge reach to 0.1m/s^2 , the damping ratio of lateral TMD achieves the optimal value, which is helpful to avoid lateral 'lock-in'.

6. FIELD VALIDATION OF CONTROL PERFORMANCE

6.1. Test of stream of pedestrians

Test of stream of pedestrians is the most direct method to assess the control system performance. By pedestrians walking freely around the main span with an increasing and controlled number up to a maximum of 400 persons, as shown in Figure 6.1, Test of stream of pedestrians was carried out. Figure 6.2 shows the recorded vertical and lateral acceleration at the middle of main span, and Figure 6.3 shows the corresponding PSDs. It can be seen from the Figure 6.2 that the lateral acceleration response increases suddenly to 0.1m/s^2 and then a beating phenomenon occurs with the acceleration in the range 0.06m/s^2 to 0.08m/s^2 , when the number of pedestrian at the main mid-span remains as 400. The PSD of vertical acceleration with 400 persons is similar to the one with

300 persons'. The several frequency peaks for the PSD of vertical acceleration in this test indicate that the step frequency is random and the 'lock-in' phenomenon does not occur.



Figure 6.1 Test of the footbridge with stream of pedestrians at central span

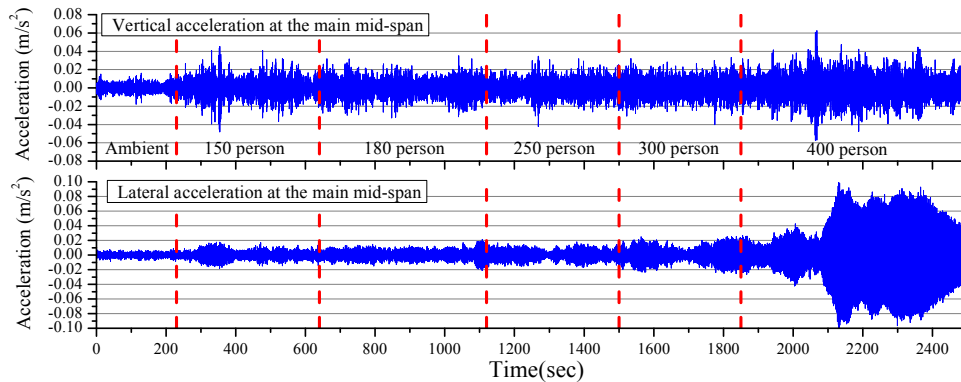


Figure 6.2 The vertical and lateral acceleration at middle of central span with stream of pedestrians

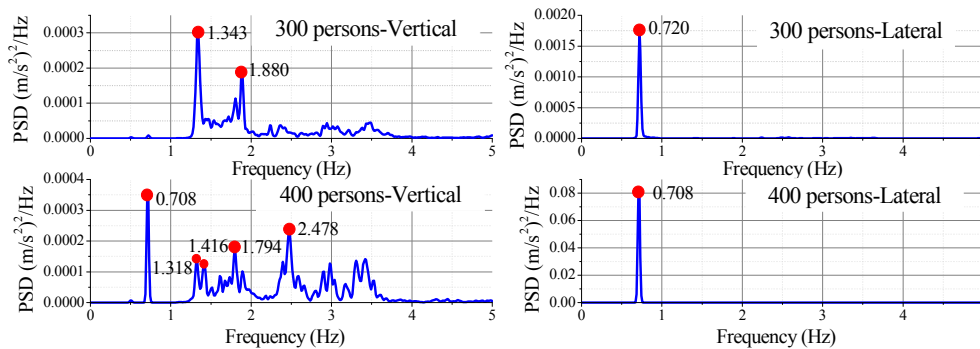


Figure 6.3 Power spectral densities of the mid-span vertical and lateral responses

6.2. Free Decay Vibration Tests

To assess the efficiencies of vertical TMDs, the damping ratios of footbridge for the three vertical control modes are estimated by free decay vibration tests. Free decay vertical acceleration responses of the footbridge and TMD unit subject to jump impulse are shown in 6.4. After jump impulse, the acceleration of the footbridge decay sharply and the equivalent damping ratios are about 5%, which are greater than the damping ratios without TMD and meet the design requirements.

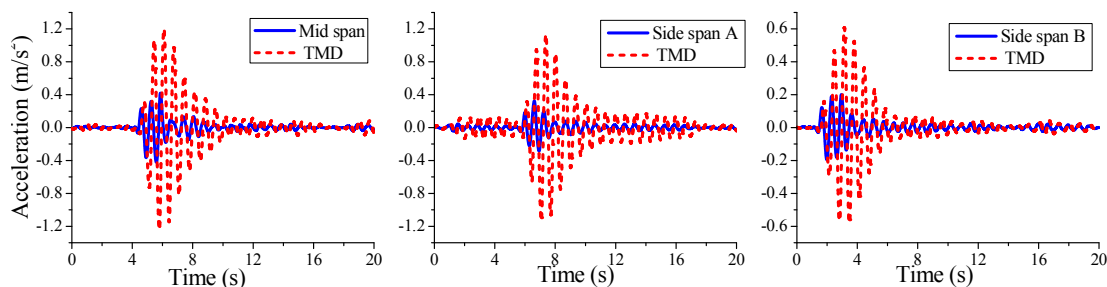


Figure 6.4 Free-decay vertical acceleration of the footbridge and TMD unit subject to jump impulse

7. CONCLUSIONS

The field validation of vibration control of a long-span cable-stayed bridge with TMDs have been presented. Ambient vibration tests, free decay vibration tests and forced vibration tests are used to determine the modal frequencies, damping ratios and modal mass of the bridge incorporated with steel link beams. Pedestrian group tests indicated that the number of pedestrians triggering synchronization lateral excitation agrees well with the theoretical one, while the measured vertical-induced responses are only about 40% the theoretical predictions of the structure under the same pedestrian density. The damping ratios for both the vertical and lateral modes increase appreciably after installation of tuned mass dampers and no evidence of large amplitude vibrations has been observed. It is important to note that the vertical TMDs operate smoothly and can be activated at small vibration amplitude while the intermittent activation of lateral TMDs has been observed which is caused by the inherent friction.

ACKNOWLEDGEMENT

The authors would like to acknowledge the support from National Science Foundation of China (Nos. 51278189, 51422806, 91215302). The collaboration of the Bureau of Municipal and Rural Construction of Mingyang, in particular Dr. Xiao-xian Kang, are of special mention. Our colleagues and PhD students, Mr. J.H. Wang, Dr. Z.H. Wang, Mr. W.X. Wang, Mr. T.F. Hu, provide great assistance to the field tests. The participation of more than 400 students from the Southwest University of Science and Technology is also acknowledged.

REFERENCES

1. Bruno L., Venuti F., and Nasce V., (2012). Pedestrian-induced torsional vibrations of suspended footbridges: proposal and evaluation of vibration countermeasures. *Engineering Structures*. **36(1)**: 228-238
2. Bendat JS PA. (1993). Engineering applications of correlation and spectral analysis. 2nd ed New York: John Wiley & Sons.
3. Brincker CV, Andersen P.. (2001). Damping estimation by frequency domain decomposition. IMAC XIX, Kissimmee, USA.
4. Caetano E, Cunha Á, Magalhães F, Moutinho C. (2010). Studies for controlling human-induced vibration of the Pedro e Inês footbridge, Portugal. Part 1: Assessment of dynamic behavior. *Engineering Structures*. **32:10**, 69-81.
5. Caetano E, Cunha Á, Moutinho C, Magalhães F. (2010). Studies for controlling human-induced vibration of the Pedro e Inês footbridge, Portugal. Part 2: Implementation of tuned mass dampers. *Engineering Structures*. **32:10**, 82-91.
6. Chen Z.Q. and Hua X. G. (2009). Dynamic Design and Control for Footbridge Vibrations. China Communications Press, Beijing.
7. Chen Z.Q., Huang Z.W., Wang J.H., Niu H.W.. (2013). Basic Requirements of Tuned Mass Damper for Bridges and the Eddy Current TMD. *Journal of Hunan University (Natural Sciences)*. **40(8)**:6-10.
8. Dallard P., Fitzpatrick T., Flint A., Le Bourva S., Low A., Ridsdill Simith R.M., and Willford M.. (2001). The London Millennium footbridge. *The Structural Engineer*. **79(22)**:17-33.
9. Footbridge_Guidelines_EN03. (2008). Design of Footbridges Guideline: Human induced Vibrations of Steel Structures. 08. September
10. Fujino Y., Pacheco B.M., Nakamura S.I., and Warnitchai P., (1993). Synchronization of human walking observed during lateral vibration of a congested pedestrian bridge. *Earthquake Engineering and Structural Dynamics*. **22(3)**: 741-758
11. Soong T.T. and Dargush G.F., (1997). Passive Energy Dissipation Systems in Structural Engineering. John Wiley & Sons, Inc, New York, NY.
12. Van O, P., De M, B. (1996). Subspace identification for linear systems: theory, implementation and applications. Dordrecht (Netherlands): Kluwer Academic Publishers.
13. Wang Z.H., Chen Z.Q.. (2013). Development and performance tests of an eddy-current tuned mass damper with permanent magnets. *Journal of Vibration Engineering*. **26(3)**:374-379. (in Chinese)
14. Wang Z.H., Hua X. G, Chen Z.Q., et al. (2014). Experimental study on vibration control of a model footbridge by a tiny eddy-current tuned mass damper with permanent magnets. *Journal of Vibration and Shock*. **32(20)**:129-32+39. (in Chinese)
15. Zivanovic S., Pavic A., and Reynolds P., (2005). Vibration serviceability of footbridges under human-induced excitation: a literature review. *Journal of Sound and Vibration*. **279(1-2)**: 1-74